PHYSICAL REVIEW C

NUCLEAR PHYSICS

Volume 25 *Third Series* Number 3

MARCH 1982

Published by

THE AMERICAN PHYSICAL SOCIETY

through the

AMERICAN INSTITUTE OF PHYSICS

$^{10}B + {}^{17}O$ fusion cross sections

Y-D. Chan,* D. E. DiGregorio,† J. L. C. Ford, Jr.,
J. Gomez del Campo, M. E. Oritz,‡ and D. Shapira
Oak Ridge National Laboratory, Oak Ridge, Tennessee 37830
(Received 8 October 1981)

The fusion cross section for $^{10}B + {}^{17}O$ has been measured at four excitation energies in ^{27}Al of $E^* = 48.4$, 55.1, 66.9, and 74.4 MeV in order to study possible compound nucleus limitation effects on fusion for light heavy-ion systems at intermediate excitation energies. Comparing this data with other measurements for different entrance channels populating the same compound nucleus it is found that for $E^* \lesssim 60$ MeV all fusion bands in the E^*-J plane of ^{27}Al appear to be parallel and displaced by the corresponding differences in separation energies, and that for $E^* > 60$ MeV the bands tend to converge indicating a possible compound nucleus limitation effect. The data are compared with existing models for entrance channel and statistical yrast line limitations.

[NUCLEAR REACTIONS $^{17}O + {}^{10}B$, $E(^{17}O) = 54$, 72, 104, and 124 MeV; measured $d^2\sigma/d\Omega dE$ for reaction products from $Z = 3$ to 12. Extracted σ_{fusion}.]

I. INTRODUCTION

The gross behavior of the complete fusion cross section for heavy-ion systems ($A_{CN} < 80$) as a function of bombarding energy can be summarized[1] as shown in Fig. 1(a). The low energy region (domain I) reflects the properties of the entrance channel potential at the barrier where potential trapping and penetration are sole prerequisites for amalgamation. The intermediate energy region (domain II) is the region where dynamical competition between fusion and peripheral reactions is expected to be important. Up until now only very limited information has been accumulated in the highest energy region (domain III) where the fusion cross section decreases drastically with increasing energy.[2] This behavior can be interpreted in terms of asymptotic properties of the compound nucleus such as the "rotating liquid-drop limit" to fusion.[2,3]

Most entrance channel model descriptions[4,5] for fusion in region II require quite specific information regarding the dynamics of the system. One example is the model of Glas and Mosel[4] where the potential strength at the critical distance, V_{cr}, is related to the slope of the fusion excitation function in region II. Even though the reduced critical distance parameter, $r_{cr}(R_{cr} = r_{cr}(A_P^{1/3} + A_T^{1/3})$, has the value of about 1.0 fm for most systems,[6] empirical values for V_{cr} extracted from experimental data do not show clear systematic trends.[4,6] It is generally believed that the fusion processes in this energy domain can be very complicated and difficult to describe.

More recently several authors[7,8] have pointed out that a simpler picture for fusion in this energy re-

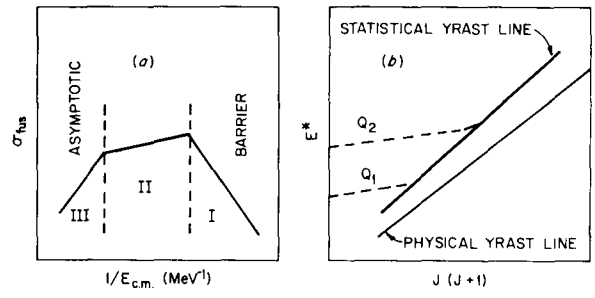

FIG. 1. (a) The gross behavior of the fusion cross section for heavy-ion reactions as a function of $1/E_{c.m}$ (based on Ref. 1) and (b) schematic illustration for the relationship between the J_{cr} trajectories corresponding to channels with different Q values (Q_1 and Q_2) populating the same compound nucleus as implied by the statistical yrast limitation model (Ref. 8).

gion could be obtained by postulating that limitations due to intrinsic properties of the compound nucleus is the actually dominating mechanism. With increasing bombarding energy the angular momenta brought into the system will eventually exceed the absorption limit of the compound nucleus and the corresponding partial waves cannot fuse. However, in order to connect the presumably simple entrance channel configuration to a more complicated CN configuration, a large and strongly intercoupled subset of levels in the E^*-J phase space at the point of injection is necessary.[7] Consequently the limitation to fusion need not by and in fact should not be the same as the physical yrast line of the nucleus. The existence of a "statistical yrast line" is suggested. In order that the concept of this effective limitation line be meaningful it should be characterized mainly by the structural properties of the compound nucleus and not by entrance channel dynamical quantities. Vandenbosch *et al.*[7] have given a detailed discussion on how to estimate the location of this line by employing the criterion that $\Gamma_J \sim D_J$ where Γ_J is the width of the compound nuclear states in the excitation region E^* and D_J is the corresponding level spacing. Lee *et al.*[8,9] have taken another approach by shifting the statistical yrast line upward in excitation energy by a constant value of ΔQ_{CN} with respect to the physical yrast line. Since the actual yrast line is not well known for light nuclei these authors have relied on the rigid rotor approximation.[8]

One interesting aspect of the "statistical yrast-line" model is that it implies a very definite relationship between the fusion cross sections for different channels populating the same compound nucleus. In the model of Lee *et al.* the fusion cross sections in region II for different entrance channels are related by[8]

$$\sigma^{\mathrm{II}}_{\mathrm{fus},i} \cong \frac{\pi \mathscr{I}_{\mathrm{CN}}}{\mu_i}\left[1+(Q_i-\Delta Q_{\mathrm{CN}})/E_{\mathrm{c.m.}i}\right], \quad (1)$$

where i is the entrance channel label, μ_i and Q_i are the corresponding reduced mass and Q value for compound nucleus formation, $\mathscr{I}_{\mathrm{CN}}$ is the moment of inertia of the compound nucleus, and ΔQ_{CN} is the statistical yrast line displacement energy. At high excitation energies the individual trajectories of the critical angular momenta for fusion of these channels should merge to coincide with the yrast limitation line of the compound nucleus [Fig. 1(b)]. This two-parameter model can be over determined, and hence tested, by studying at least three different channels populating the same compound nucleus. Such a test is the main motivation of the present measurement.

The $^{10}B + {}^{17}O$ system populates the compound nucleus ^{27}Al. It can be seen from Table I that this channel has a much higher Q value for compound nucleus formation (28.4 MeV) than the other systems ($^{13}C + {}^{14}N$, $^{11}B + {}^{16}O$, $^{12}C + {}^{15}N$) readily available for experiment. The $^{10}B + {}^{17}O$ channel is also unusual in that the ground state spins for both nuclei are quite large ($\frac{5}{2}^+$ and 3^+) as compared to other nuclei in this mass region. Consequently the entrance channel spin can be as high as $\frac{11}{2}$ units of $\hbar$ which is a substantial fraction of the grazing orbital angular momentum ($\sim 20-30\hbar$) at the energies of the present study.

It should be noted that for systems with nonzero entrance channel spin, two different values for the critical angular momentum can be extracted from the experimental data (by the sharp cutoff model for fusion) depending on whether one requires the cutoff on the orbital angular momentum (l_{cr}), or on the total angular momentum (J_{cr}). In the first case, the result is identical to that of the spin-0 case, namely,

$$(l_{\mathrm{cr}}+1)^2 \equiv \sigma^{\mathrm{exp}}_{\mathrm{fus}}/\pi\lambda\!\!\!^{-2} . \quad (2)$$

In the latter case, however, one would have instead

TABLE I. Heavy-ion entrance channels populating the compound nucleus ^{27}Al.

Channel	Q_{CN} (MeV)	Channel spin	$(S_{\max})$ $(\hbar)$
$^{10}B + {}^{17}O$	28.4	$3^+, \frac{5}{2}^+$	(5.5)
$^{13}C + {}^{14}N$	23.2	$\frac{1}{2}^-, 1^+$	(1.5)
$^{11}B + {}^{16}O$	21.1	$\frac{3}{2}^-, 0^+$	(1.5)
$^{12}C + {}^{15}N$	17.2	$0^+, \frac{1}{2}^-$	(0.5)

$$\sigma_{\text{fus}}^{\text{exp}} \equiv \sum_{J=0}^{J_{\text{cr}}} \sigma_J \,,$$

$$\alpha_J = \frac{(2J+1)\pi\lambda^2}{(2I_1+1)(2I_2+1)} \times \sum_{I=|I_1-I_2|}^{I_1+I_2} \sum_{l=|J-I|}^{J+I} \theta(l_g - l) \,, \tag{3}$$

where θ is the usual step function, I_1, I_2 are the spins of the projectile and target nuclei, I is the channel spin, l is the orbital angular momentum, and l_g denotes the entrance channel grazing angular momentum. The constraint $l < l_g$ assures that only partial waves smaller than the grazing partial wave can contribute to complete fusion. This condition is shown explicitly in (3) so that for $J < J_{\text{cr}}$, terms with $l = J + I$ larger than l_g are not included. Results obtained from (2) are often quoted in the literature for systems with nonvanishing channel spins even though we think that the J_{cr} values from (3) are more appropriate for comparison concerning compound nucleus limitation effects. It is nevertheless true that the difference between l_{cr} and J_{cr} is usually very small and is important only at low energies.

II. EXPERIMENT

The measurements were performed with the MP-Tandem of the Brookhaven National Laboratory Tandem Facility at beam energies of E_{lab} (^{17}O) = 54, 72, 104, and 124 MeV. The fusion cross sections were deduced by integrating the measured angular distributions of the heavy residues.

A. Experimental setup

The experimental setup is shown in Fig. 2. The main detector was a particle telescope comprised of an ionization chamber ΔE counter and a position sensitive silicon counter (~ 1000 μm thick) as the E detector. Entrance windows for the ionization chamber were made of stretched polyproplane foils ~ 80 μg/cm^2 thick and pure methane gas (14–20 Torr) was used as the detector gas. The ΔE and E signals were gain matched by means of an α source and summed to yield the total energy signal. An angle defining slit mask was positioned in front of the telescope so that four angles could be measured simultaneously. The slits were separated by 2.0 $\pm$ 0.1° and each slit subtended an in-plane acceptance

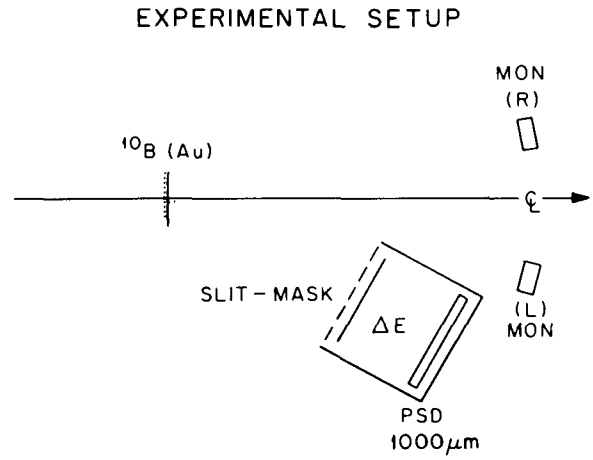

FIG. 2. Experimental setup for the ^{10}B + ^{17}O measurement.

angle of 1.8°. The solid angle of the individual slits (~ 0.4 msr) was determined by a calibrated α source. Two monitor detectors were mounted symmetrically on either side of the beam to provide additional monitoring and relative normalization information. The detectors were aligned with respect to the beam axis with an optical telescope with an estimated accuracy of $\sim$ 0.1°.

The target was composed of an isotopic ^{10}B (97%) self-supporting foil ~ 50 μg/cm^2 in areal density. A flash of gold ~ 1 μg/cm^2 thick had been evaporated onto the beam side of the target in order to obtain the absolute normalization of the cross sections. The ^{10}B to Au target thickness (in μg/cm^2) ratio, R, was 1:0.0275 as determined by Rutherford scattering at E_{lab} (^{17}O) = 20 MeV at forward angles. Due to the target fabrication process there was an approximately 8% oxygen contaminant in the target. The consequences of this contamination and the procedure we have applied to correct the experimental data will be described in Sec. III.

B. Data acquisition

The measurements were conducted in singles mode with a valid telescope event comprised of three parameters; the position P, ΔE, and E_T ($\equiv \Delta E + E$). The position signal was obtained by an analog divider which has an E-pulse threshold of ~ 50 mV. Software gates were drawn on the P vs E_T spectrum to generate four ΔE-E_T maps each of which corresponded to a single detection angle. The events were sorted on line according to the po-

sition. Sample two-dimensional spectra for P vs E_T and ΔE vs E_T are shown in Figs. 3 and 4. Both the position resolution and charge separations were sufficient for our purpose. The bending of the position bands at low E signals (Fig. 3) caused by the nonlinear response of the detector and analog divider were taken care of by drawing the two-dimensional gates accordingly.

C. Absolute normalization

The Coulomb scattering of ^{17}O on Au together with the measured ^{10}B to Au target thickness provided the absolute normalization for our data. Besides avoiding the uncertainties usually associated with the absolute target thickness and beam current integration, this method of normalization is necessary in our case as the beam current was blocked by the physical size of the telescope for the most forward angle measurements. By aligning the detector angles accurately the uncertainty in the absolute cross section due to this normalization procedure was estimated to be $\sim 5\%$.

III. DATA REDUCTION

There were two major problems in extracting the fusion cross sections for the present experiment.

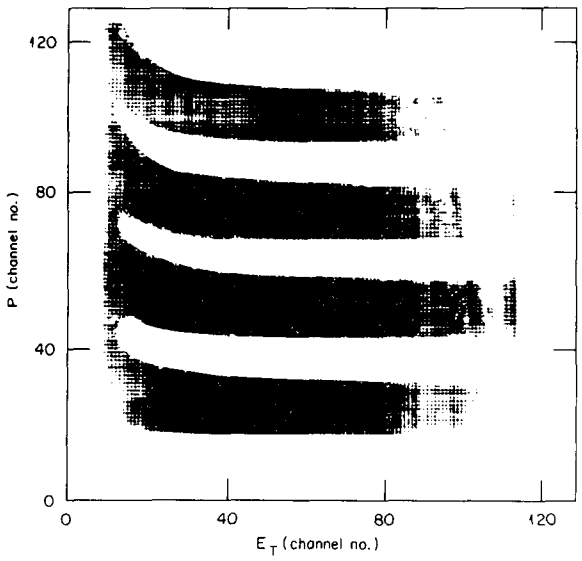

FIG. 3. Position versus total energy spectrum taken at $\theta_{lab}=10°$ and $E_{lab}(^{17}O) = 124$ MeV.

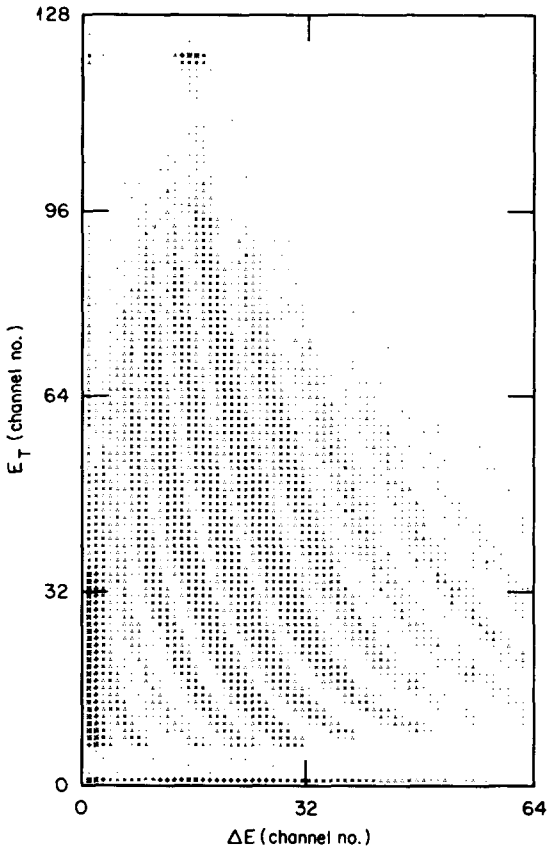

FIG. 4. Two-dimensional ΔE-E_T map for a single slit. The spectrum was taken at $\theta_{lab}=15°$ and E_{lab} (^{17}O) = 124 MeV.

The first is due to the strong overlapping of the peripheral reaction and fusion residue components in the energy spectra for residues with Z values close to that of the beam. This difficulty is inherent to fusion measurements in this mass region. Figure 5 shows the residue yield pattern for $^{10}B + {}^{17}O$ (124 MeV) estimated by the Monte Carlo evaporation code LILITA.[10] It can be seen that the yield strength is dominated by atomic numbers close to that of the beam. Spectrum decomposition is necessary in this case to separate out the direct components.[2] Another problem is the oxygen contamination in the target. The fusion of $^{16}O + {}^{17}O$ will also produce residues close to our region of interest. By assuming an identical cross section as for ^{10}B and an 8% oxygen contaminant the Z yield pattern for $^{16}O + {}^{17}O$ is shown by the blank histogram in Fig. 5. Residues with atomic number $Z=8$ and up are affected. To remedy both these problems we have relied on evaporation model spectra simulations in guiding the data reduction process.

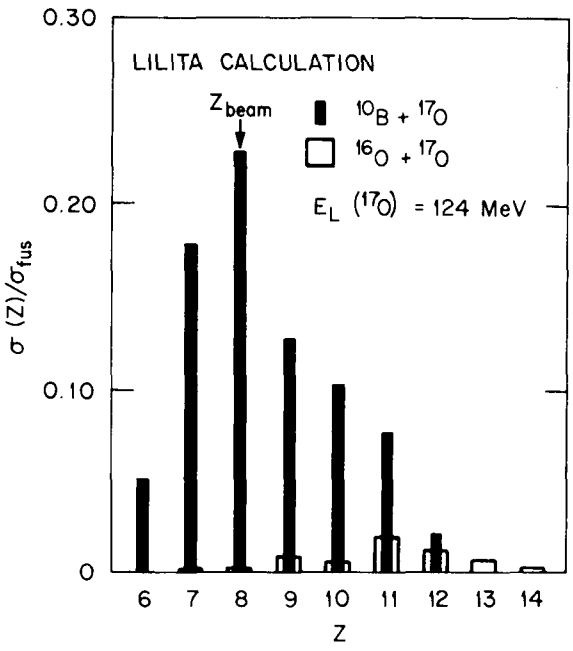

FIG. 5. Estimation of the effect of the oxygen contamination ($^{16}O + ^{17}O$) in the target on the residue yields at E_{lab} (^{17}O) = 124 MeV. Identical fusion cross sections for ^{16}O and ^{10}B, and an 8% oxygen contaminant were assumed.

A. Spectra decomposition

To decompose the energy spectra into peripheral and compound components, the energy centroids and widths of the residue yields in the laboratory system were simulated with the code LILITA.[10] Figure 6 shows the comparison between the experimental and calculated energy spectra at E_{lab} (^{17}O) = 124 MeV where mixing is expected to be the strongest. The calculations were arbitrarily normalized to the experiment for each Z. For residues with $Z > 10$ the agreement between data and calculations is good and no decomposition was necessary. However, substantial subtractions had to be made for elements with $Z = 9$ and smaller. The good agreement between calculations and data for high Z residues gave us confidence in the reliability of this extraction procedure. It is probably also the only way for extracting fusion cross sections in this mass region without evoking more exclusive coincidence measurements.

It should be noted that only the calculated peak centroids and widths were used in the data reduction process but not the predicted yields. Therefore

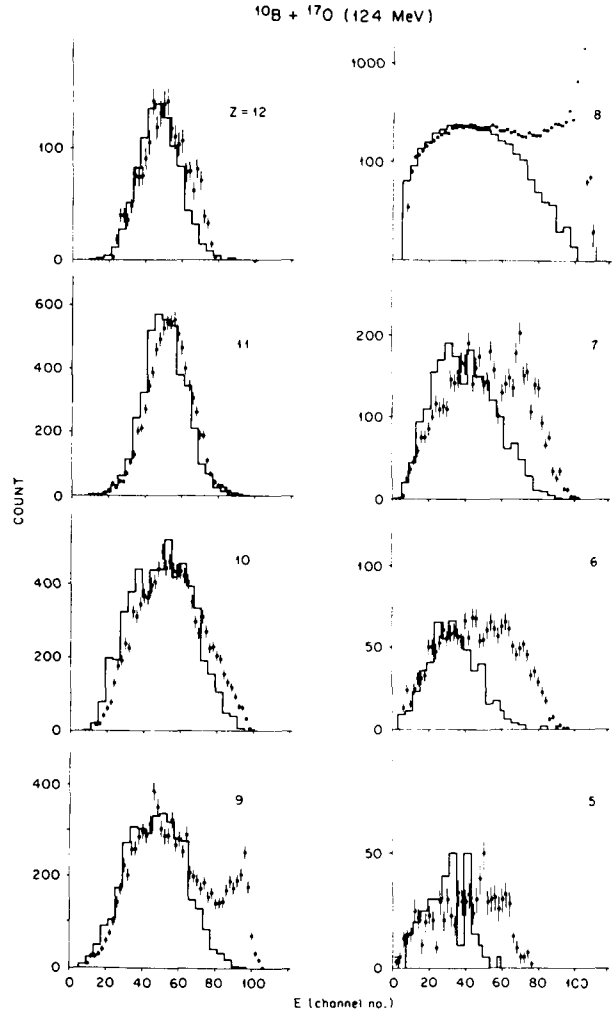

FIG. 6. An example of decomposing the residue energy spectra into compound and peripheral components. The histograms were generated by the Monte Carlo code LILITA.

our analysis is model dependent in the kinematic sense but not on the details of the parameters used in the calculation. In fact the calculated peak centroids and widths were not sensitive to the statistical model parameters.

It is interesting to note that two distinct components could also be observed in some of the energy spectra for high Z residues (e.g., Ne) at forward angles and at low bombarding energies (Fig. 7). These components, however, appear to be of kinematical origin corresponding to the difference in recoil energy of the residue when accompanied by forward and backward α emission. No decomposition was needed. To examine this effect calculations were performed to separate the residue yields into two parts corresponding to backward (B) or

forward (F) light particle emission (Fig. 7). The result agrees well with the experimental observation and supports the previous statement. Similar effects were not observed for residues accompanied only by nucleon emissions (e.g., Mg) due to the smaller light particle mass.

B. Correction for oxygen contaminant

Since the energy centroid of a given residue from the $^{16}O + ^{17}O$ reaction usually lies lower in energy than that resulting from $^{10}B + ^{17}O$, and as the contaminant reaction contribution is usually small and does not form distinct peaks, the energy decomposition method becomes less useful. To correct the data we have made use of the fact that to reach the same final daughter nucleus the ^{33}S ($^{16}O + ^{17}O$) compound nucleus has to emit six more nucleons than does ^{27}Al ($^{10}B + ^{17}O$). Consequently the angular distribution for the ^{33}S residues has a much wider spread in angle. An example is shown in Fig. 8 comparing the calculated Mg ($Z = 12$) yields from both reactions at E_{lab} (^{17}O) = 54 MeV. It can be

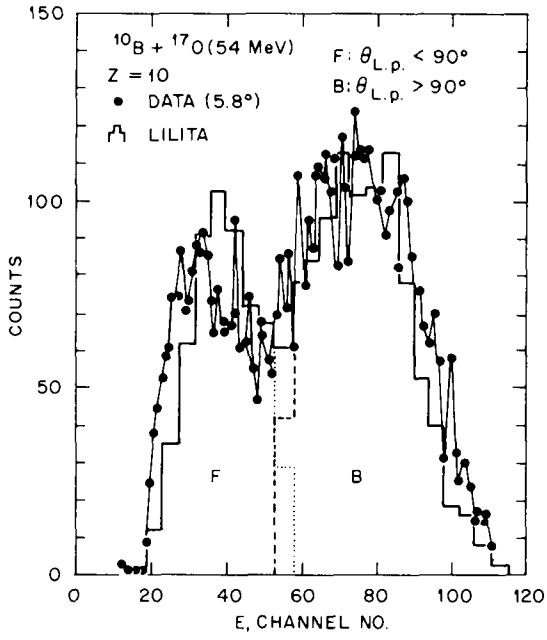

FIG. 7. The kinematical origin of the two components observed in the $Z = 10$ yield at $\theta_{lab} = 4.8°$ and E_{lab} (^{17}O) = 54 MeV. The histograms are results of the LILITA calculation sorted according to forward (F) or backward (B) particle emission.

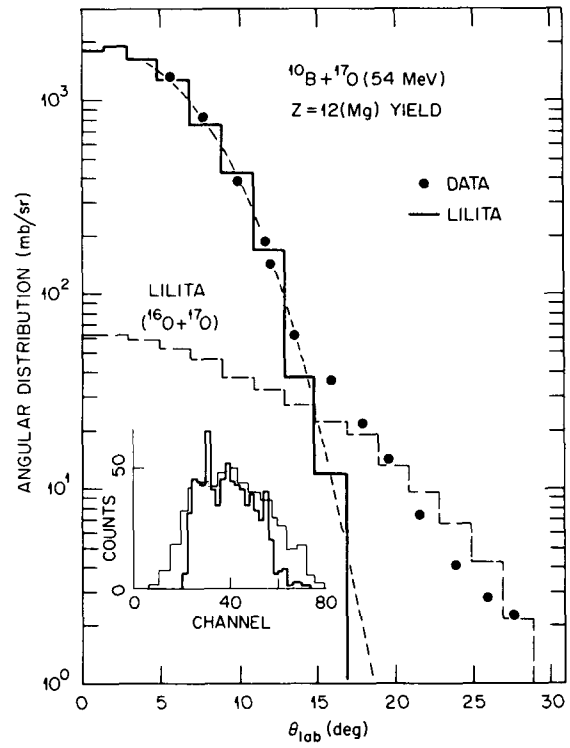

FIG. 8. An example of subtracting the oxygen contamination yield by normalizing the calculated angular distribution at large angles to the experimental yield. The inset shows the calculated Mg energy spectrum originating from the $^{16}O + ^{17}O$ reaction as compared with the measured spectrum (heavy lined histogram) at $\theta_{lab} = 20°$.

seen that for $\theta_{lab} > 20°$, the code predicts essentially no yield (within the statistics of the Monte Carlo calculation) for the $^{10}B + ^{17}O$ reaction while the experimental angular distribution agrees well with the calculation for $^{16}O + ^{17}O$ at large angles. The comparison of the experimental and calculated energy spectra at $\theta_{lab} = 20°$ for the Mg residual is shown in the inset of Fig. 8. Both support the interpretation that all the 20° counts actually come from the oxygen target contaminant. The experimental cross section was corrected by normalizing the calculated angular distribution to the raw data at large angles and subtracting off the integrated yield.

The amount subtracted, due to the oxygen contamination, from the individual residue lies between 3–5 % and is smaller than the uncertainties associated with the spectrum decomposition process. The uncertainty in the total fusion cross section arising from the higher Z residues is even smaller since they contribute only a small fraction of the total residue yield.

IV. RESULTS

The results of the measurement are summarized in Table II. The largest fusion cross section we have observed is 1250 ± 110 mb for the 104 MeV data point. The uncertainties are estimated to be ~ 7% for the two lowest energy points and ~ 9% for the two higher energy points. Also listed are the critical angular momenta values l_{cr} and J_{cr} extracted from the data by using the sharp cutoff model according to Eqs. (2) and (3), assuming the transmission coefficients are independent of the channel spins.

The percentage residue yield as a function of Z at different bombarding energies as well as the evaporation model calculations are shown in Fig. 9. The LILITA calculations (shown by blank histograms) were performed with statistical model parameters obtained either by fitting the known low-lying levels of the nuclei or from the systematic study of Ref. 11. Generally speaking, the yield for the higher Z residues can be well reproduced by the code, even though large discrepancies exist for residues lying below the beam. These low Z residues usually correspond to the late stages of the deexcitation process where particles are emitted from a relatively low excitation region of the parent nuclei. The accuracy of the calculation may have been affected by the approximations employed in treating the level density and transmission coefficients at low excitation energies.[10]

The comparison of the l_{cr} values from the present work to those of Wieleczko *et al.*[12] for $^{10}B + {}^{17}O$ is shown in Fig. 10. Also included are other known experimental results for the related channels $^{13}C + {}^{14}N$, $^{11}B + {}^{16}O$, and $^{12}C + {}^{15}N$ taken from the literature.[12,13] The agreement of our 54 and 72 MeV data with the Saclay work is good. The 124 MeV data point also lies within an error bar to the points for $^{13}C + {}^{14}N$ and $^{11}B + {}^{16}O$ measured at approximately the same excitation energy. At these energies, l_{cr} and J_{cr} are almost identical and the close promixity of the l_{cr} values for at least three channels at E^* (^{27}Al) > 70 MeV supports the statistical yrast limit picture.

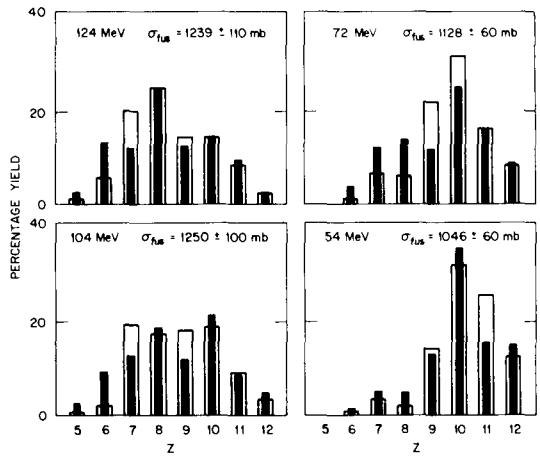

FIG. 9. Experimental percentage residue yields for $^{10}B + {}^{17}O$ (solid histograms) compared with LILITA calculations (blank histograms).

V. ENTRANCE CHANNEL MODEL CALCULATIONS

To examine the data further we have performed some simple model calculations for the fusion cross sections induced by the four channels shown in Fig. 10. Even though the original motivation was to study the compound nucleus-limitation effects on fusion, it is interesting to see how well the entrance channel models can reproduce the data.

According to the model of Glas and Mosel the fusion cross sections in domains I and II are given by[4]

$$\sigma_{fus}=\pi\lambda^2\sum_{l=0}^{l_{cr}}(2l+1)\{1+\exp[2\pi(V_{Bl}-E)]/\hbar\omega)\}^{-1},$$

$$V_{Bl}=V_B+\hbar^2 l(l+1)/(2\mu R_B{}^2), \tag{4}$$

$$l_{cr}(l_{cr}+1)=2\mu R_{cr}{}^2(E-V_{cr})/\hbar^2,$$

TABLE II. Summary of experimental results for $^{10}B + {}^{17}O$ in the present measurement.

E_{lab} (MeV)	$E_{c.m.}$ (MeV)	E^*_{CN} (MeV)	σ_{fus} (mb)	l_{cr} ($\hbar$)	J_{cr} ($\hbar$)
54	20.0	48.4	1046±60	13.2	14.1
72	26.7	55.1	1128±60	16.0	16.7
104	38.5	66.9	1250±110	20.5	20.5
124	45.9	74.4	1239±110	22.4	22.4

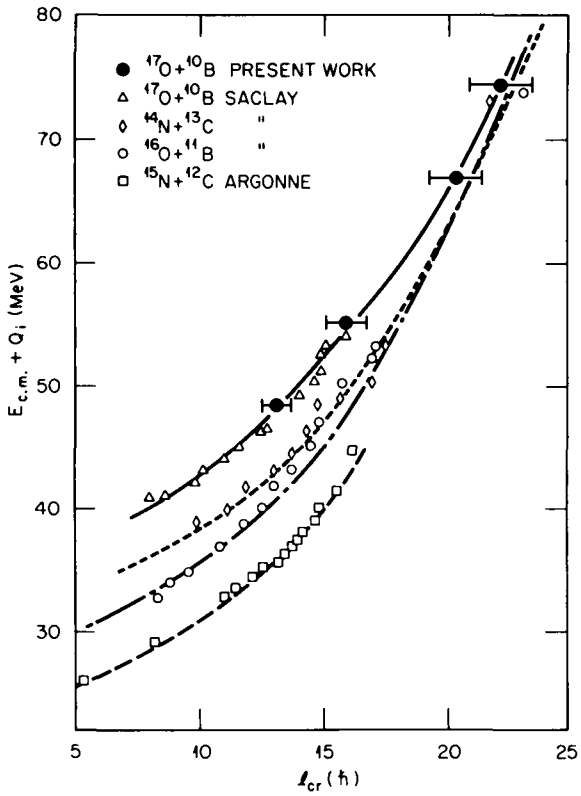

FIG. 10. Summary of existing fusion data for the ^{27}Al system. The curves are Glas-Mosel model calculations.

where $R_{cr}(R_B)$ and $V_{cr}(V_B)$ are the critical (barrier) radii and potential strengths. The l_{cr} values corresponding to fusion cross sections calculated by the Glas-Mosel model are shown by different curves in Fig. 10 and the parameters used in the calculations are tabulated in Table III. The l_{cr} values were obtained from the experimental data by use of Eq. (2). The trend of the data at low excitation energies for all channels can be well reproduced by using almost identical barrier parameters. This is consistent with the picture that at low energies the fusion systematics follow basically the geometrical scaling of the entrance channel. The separation of the trajectories in this region is simply due to the different Q_i values of the individual channels.

However, in order to describe the data at higher excitation energies [$E^*(^{27}Al) > 60$ MeV], the $^{10}B + {}^{17}O$ channel requires a relatively large r_{cr} value of 1.28 fm. The r_{cr} value needed for $^{13}C + {}^{14}N$ and $^{11}B + {}^{16}O$, $r_{cr} = 1.20$ fm, is also larger than the nominal value of 1.0 fm.[6] For comparison, the parameters for $^{10}B + {}^{16}O$ and $^{12}C + {}^{14}N$ (which populate the compound nucleus ^{26}Al and differ from the present system by only a single neutron) are also listed in Table III. It is interesting to notice the similarity between these two systems in that the channel with the highest Q_i value also requires the largest r_{cr} value. It is conceivable that even though kinematical matching conditions are comparable, the larger compound nucleus phase space seen by the channel with the higher Q_i may be reflected as an increase in r_{cr} in the entrance channel description for lighter systems.

VI. COMPOUND NUCLEUS LIMITATION MODELS

Compound nucleus limitations on fusion cross sections are described by the models of Vandenbosch *et al.*[7] and Lee *et al.*[8] For the sake of clarity only the data for the $^{10}B + {}^{17}O$ and $^{12}C + {}^{15}N$ channels, together with a high energy data point for the $^{13}C + {}^{14}N$ reaction at $E^*(^{27}Al) = 98$ MeV,[12] are plotted against $J(J+1)$ in Fig. 11. This provides a wide dynamical range for comparison.

Kolata[14] has pointed out that the fusion cross sections for $^{16}O + {}^{16}O$, $^{12}C + {}^{12}C$, and $^{16}O + {}^{12}C$ at high energies appear to be limited by the extrapolated ground state band of the compound nucleus. The dotted curve in Fig. 11 shows the extrapolated ground state band for ^{27}Al based on known low-lying levels. It can be seen that this band is not limiting the present system.

The results of the model calculations are shown

TABLE III. List of parameters used in the Glas-Mosel model calculations.

Channel	r_B (fm)	V_B (MeV)	r_{cr} (fm)	V_{cr} (MeV)	$\hbar\omega$ (MeV)
$^{10}B + {}^{17}O$	1.5	6.7	1.28	0.0	2.0
$^{13}C + {}^{14}N$	1.5	6.7	1.20	1.0	2.0
$^{11}B + {}^{16}O$	1.5	7.7	1.20	0.0	2.0
$^{12}C + {}^{15}N$	1.5	6.7	1.20	0.0	2.0
$^{10}B + {}^{16}O$	1.5	6.7	1.35	2.5	2.0
$^{12}C + {}^{14}N$	1.5	6.7	1.11	−1.9	2.0

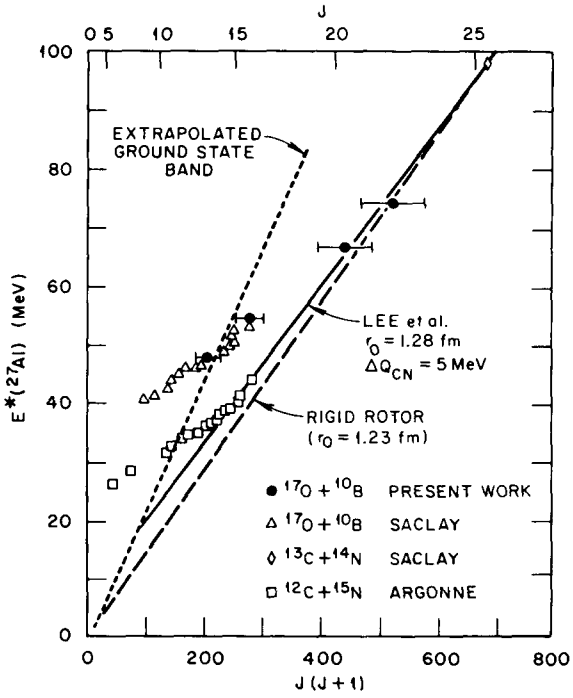

FIG. 11. Statistical yrast limitation calculations according to the model of Ref. 8.

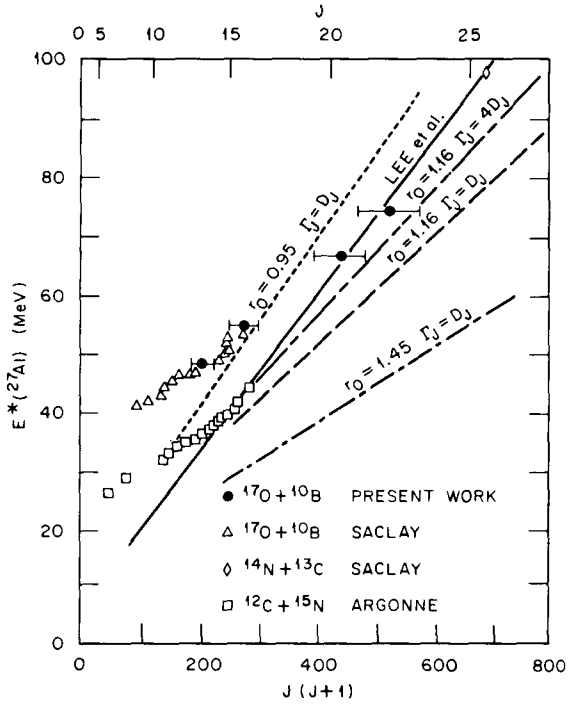

FIG. 12. The location of the statistical yrast line for the ^{27}Al nucleus as estimated by the model of Vandenbosch *et al.*[7]

in Figs. 11 and 12. Due to the uncertainties associated with the data the parameters could not be unambiguously determined. In fact, the high energy data points can be fitted quite well by a simple rigid rotor model with $r_0 = 1.23$ fm (dashed curve, Fig. 11). But since this curve misses the saturated region of the $^{12}C + ^{15}N$ channel a more reasonable fit based on the model of Ref. 8 can be obtained as shown by the heavy solid curve in Fig. 11. The parameters, $r_0 = 1.28$ fm and $\Delta Q_{CN} = 5$ MeV, differ quite significantly from the values of 1.20 fm and 10 MeV deduced by Lee *et al.*[8] for other systems.

The model of Lee *et al.*[8] only provides a parametrized form of the statistical yrast line trajectory. To see if the parameters deduced are physically reasonable we have estimated the location of the limiting trajectory for ^{27}Al according to the model of Vandenbosch *et al.*[7] In this model, the criterion for a partial wave l, corresponding to channel spin S and total angular momentum J, to be absorbed by the compound nucleus is that $\Gamma_J \sim D_J$ where Γ_J is the local compound nuclear level width and D_J is the corresponding level spacing. The parameters suggested by Vandenbosch *et al.*[7] were used. The average level spacing was calculated using the back-shifted Fermi gas model[15] with the rigid rotor spin cutoff parameter $r_0 = 1.16$ fm and Γ_J was calculated by the J-independent empirical formula of Shapira *et al.*,[16]

$$\Gamma_J = 14 \exp(-4.69S) , \qquad S = (A/E^*)^{1/2} , \tag{5}$$

where A is the atomic number of the nucleus and E^* the excitation energy. The level density and pairing energy parameters were obtained from Ref. 15. The result, shown by the long dashed curve labeled $r_0 = 1.16$ and $\Gamma_J = D_J$ in Fig. 12, does not have the same slope as the higher energy portion of the data. For comparison, the calculated curve corresponding to the requirement that $\Gamma_J = 4D_J$ is also plotted (dotted-dashed curve). Even though this latter curve lies closer to the data in excitation energy, the slope of the empirical trajectory is still not reproduced. Changing the r_0 parameter drastically from $r_0 = 1.16$ to 0.95 fm generates a trajectory (short-dashed curve) whose slope is much closer to that of the empirical line but lies too high in excitation energy.

These calculations were found to be not very sensitive to variations in the level density parameter a. It should be noted, however, that Γ_J is independent of J due to the approximations made above and this

fact may have affected the results. The spin cutoff parameter for ^{27}Al has also been deduced by Gomez del Campo *et al.*[17] by studying α emission from the $^{12}C + {}^{15}N$ reaction. The value reported,[17] $r_0 = 1.45$ fm, is substantially different from that suggested by Ref. 7. The calculated curve corresponding to this value is shown by the dotted-dashed line in Fig. 12 which deviates even further from the data. These discrepancies are most likely due to lack of accurate information on Γ_J and D_J and do not necessarily invalidate the criterion $\Gamma_J \sim D_J$ which seems physically very acceptable. However, these problems indicate that caution should be exercised in comparing this model to experimental results.

VI. SUMMARY

We have extended the complete fusion cross section measurements for $^{10}B + {}^{17}O$ to $E^*(^{27}Al) \sim 75$ MeV. The low energy points agree well with those of Ref. 13. These measurements and existing fusion data for $^{13}C + {}^{14}N$ and $^{11}B + {}^{16}O$ at high excitation energies[12,13] yield values for J_{cr} (fusion) that appear to approach a common trajectory. This trend is consistent with the existence of a compound nucleus limitation on the fusion cross section at high excitation energies of ^{27}Al. Data points are scarce in this energy region, however, and results for the $^{12}C + {}^{15}N$ channel are still unavailable. It would be very desirable to have high energy $^{12}C + {}^{15}N$ measurements to fill in this gap.

ACKNOWLEDGMENTS

We thank Dr. P. D. Bond and the supporting staff of the BNL tandem facility for their help at various stages of the experiment, and to Dr. Y. Kondo for his discussion on the role of l_{cr} and J_{cr}. This work was supported by the Oak Ridge National Laboratory operated by Union Carbide Corporation under Contract W-7405-eng-26 with the U. S. Department of Energy.

---

*Present address: Lawrence Berkeley Laboratory, Berkeley, California 94720.

†On leave of absence from Comision Nacional de Energia Atomica, Buenos Aires, Argentina.

‡Present address: Instituto de Fisica, Universidad Nacional Autonoma de Mexico, Mexico 20, D.F., Mexico.

[1]R. G. Stokstad, Proceedings of the Topical Conference in Heavy-Ion Collisions, Fall Creek Falls, Tennessee, 1977, edited by E. C. Halbert, J. A. Maruhn, V. Maruhn-Rezwani, and J. B. McGrory, CONF 770602, p. 22.

[2]J. Gomez del Campo, R. A. Dayras, J. A. Biggerstaff, D. Shapira, A. H. Snell, P. H. Stelson, and R. G. Stokstad, Phys. Rev. Lett. 43, 26 (1979).

[3]S. Cohen, F. Plasil, and W. J. Swiatecki, Ann. Phys. (N.Y.) 82, 557 (1974).

[4]D. Glas and U. Mosel, Nucl. Phys. A237, 429 (1975).

[5]J. R. Birkelund, L. E. Tubbs, J. R. Huizenga, J. N. De, and D. Sperber, Phys. Rep. C56, 107 (1979).

[6]J. Gallin, D. Guerreau, M. Lefort, and X. Tarrago, Phys. Rev. C 9, 1018 (1974).

[7]R. Vandenbosch and J. Lazzarini, Phys. Rev. C 23, 1074 (1981).

[8]S. M. Lee, T. Matsuse, and A. Arima, Phys. Rev. Lett. 45, 165 (1980).

[9]S. M. Lee, Y. Higashi, Y. Nagashima, S. Hana Shima, M. Sato, H. Yamaguchi, and M. Yamanouchi, Phys. Lett. 98B, 418 (1981); T. Matuse, A. Arima, T. Tsukamoto, and S. M. Lee, contributed paper to the Proceedings of the International Conference on Nuclear Physics, Berkeley, 1980, Lawrence Berkeley Laboratory Report No. LBL-11118.

[10]J. Gomez del Campo and R. G. Stokstad, Oak Ridge National Laboratory Report ORNL-TM-7295, 1981.

[11]U. Facchini and E. Saetta-Menichella, Energ. Nucl. (Milan) 15, 54 (1968).

[12]J. P. Wieleczko, S. Harar, M. Conjeaud, and F. Saint-Laurent, Phys. Lett. 93B, 35 (1980).

[13]D. G. Kovar, D. F. Geesman, T. H. Braid, Y. Eisen, W. Henning, T. R. Ophel, M. Paul, K. E. Rehn, S. J. Sanders, P. Sperr, J. P. Schiffer, S. L. Tabor, S. Vigdor, B. Zeidman, and F. W. Prosser, Jr., Phys. Rev. C 20, 1305 (1979).

[14]J. J. Kolata, Phys. Lett. 95B, 215 (1980).

[15]A. Gilbert and A. G. W. Cameron, Can. J. Phys. 43, 1446 (1965).

[16]D. Shapira, R. G. Stokstad, and D. A. Bromley, Phys. Rev. C 10, 1063 (1974).

[17]J. Gomez del Campo, J. L. C. Ford, Jr., R. L. Robinson, M. E. Oritz, A. Dacal, and E. Andrade, Nucl. Phys. A297, 125 (1978).

PHYSICAL REVIEW C

Postmaster: If undeliverable, send notice on Form 3579 to:

American Institute of Physics
335 East 45th Street
New York, N.Y. 10017

SECOND CLASS POSTAGE PAID AT WOODBURY, N.Y. AND ADDITIONAL MAILING OFFICES

For editorial and subscription correspondence, please see inside front cover

ISSN: 0556-2813

THIRD SERIES, VOLUME 25, NUMBER 3 *CONTENTS* MARCH 1982

Nuclear Reactions

Heavy Ions

(Continued)